

PAPER • OPEN ACCESS

Study on experiment and finite element modelling of small punch test

To cite this article: Xianlong Zhang *et al* 2019 *IOP Conf. Ser.: Mater. Sci. Eng.* **544** 012051

View the [article online](#) for updates and enhancements.



IOP | ebooks™

Bringing you innovative digital publishing with leading voices to create your essential collection of books in STEM research.

Start exploring the collection - download the first chapter of every title for free.

Study on experiment and finite element modelling of small punch test

Xianlong Zhang¹, Zhaonan Ding¹, Yuguang Chen¹, Liqing Zhang¹ and Chonghong Zhang¹

¹ Institute of Modern Physics, Chinese Academy of Sciences. Lanzhou, China.
E-mail: zhang.xl@impcas.ac.cn

Abstract. The small scale specimen techniques have been a fast-growing research field for the past three decades. Small punch test is the most commonly used small specimen test technology and numerous mechanical properties are obtained from the test. Due to the highly complex stress state of the sample during the experimental process, many empirical formulas are used to obtain mechanical properties of the specimen. The curve obtained by finite element modelling of the small punch test is quite different from that obtained from the experiment, this paper present a systematic study on the problem. A revised model is proposed to solve the issue and we conclude that the rod must be modelled in the finite element simulation and the deformation of the rod is the causes of the misaligned.

1. Introduction

Small-scale specimen techniques attract considerable attention nowadays. Over the past three decades, numerous techniques for non-standard small samples have been established to characterize mechanical and physical properties. Small-scale specimen techniques are firstly used in the nuclear industry due to the limitation of irradiation space in the reactor and the dose to testers for post-irradiation testing[1, 2]. Small punch test (SPT) is the most widely used to extract the fracture properties among all the small-scale test techniques, since SPT only requires a thin slice ($\varnothing 8 * 0.5\text{mm}$ or even $\varnothing 3 * 0.3\text{ mm}$) of material to assess materials properties of an in-service component.

Researchers proposed empirical relation between tensile yield stress and the inflection point of the SPT load-deflection curve as well as between the maximum load of the SPT curve and the ultimate tensile stress based on their own experimental results. SPT has also been employed to non-nuclear industries such as pressure vessel and fossil fuel energy production plants[3]. SPT has been extended to evaluate mechanical properties including ductility, fracture toughness, creep behaviour and ductile to brittle transition temperature. Four different stage were identified in a typical SPT load-deflection curve, the four consecutive regime are: (1) elastic bending of the specimen, (2) plastic bending of the disk followed by membrane stretching (3) and, finally, (4) local crack formation. However, it is important to mention that the boundaries between different stages are difficult to identify.

Assessing SPT apparatus parameters on the load-deflection curve is necessary for understanding this technique, Lucas et al[4] systematically investigated the effect of specimen thickness, clamp apparatus size and materials through experiment. Moreno investigate the influence of different displacement measurement method on the experimental results [5]. Campitelli[6, 7] investigated the effect of yield stress, friction coefficient and compliance of the load system by finite element method (FEM) combining with experiment. Due to the higher complexity of the stress state of SPT, the mechanical properties can not be obtained directly from the load-deflection curve of the test and FEM was used to simulate the experiment in the present work.



However, a significant issue is often ignored, this is the load-deflection curve obtained by the FEM simulation disagree with the experimental curve. There are still no systematic studies on this issue and only few authors corrected the FEM simulation curve by adding the compliance of the system. In the present work, a through study is performed with the aim of clarifying this issue. It includes revision of traditional FEM modelling of the rigid loading system of SPT, the loading system compliance and discussion on the permanent plastic deformation of the loading system.

2. Experiment details

2.1. Material employed

The material employed in this study is low carbon content austenitic stainless steel 316L, commercial steel provided by Goodfellow Company, its nominal composition is listed in Table 1.

Table 1. Composition of austenitic SS316L. (wt%)

Cr	Ni	Mo	Mn	Si	S	C	Fe
17	12	2.5	2	1	0.03	0.03	65.44

2.2. Uniaxial tensile test

Uniaxial tensile test is performed at room temperature. Sheet specimen with a width of 12.5mm, length of parallel section of 65mm, thickness of 0.5mm, and gauge length of 150mm is used for uniaxial tensile test, presented in figure 1. The electro-mechanical testing machine is controlled at a constant crosshead velocity to make sure the strain rate of 0.015 s^{-1} , which is nearly the strain rate of the first stage of the small punch test. Note that the strain rate varies of different stage of the SPT experiment. The elongation of the interest section is measured by clip gauge attached to the sample. The nominal and the true stress-strain curve are presented in figure 2.

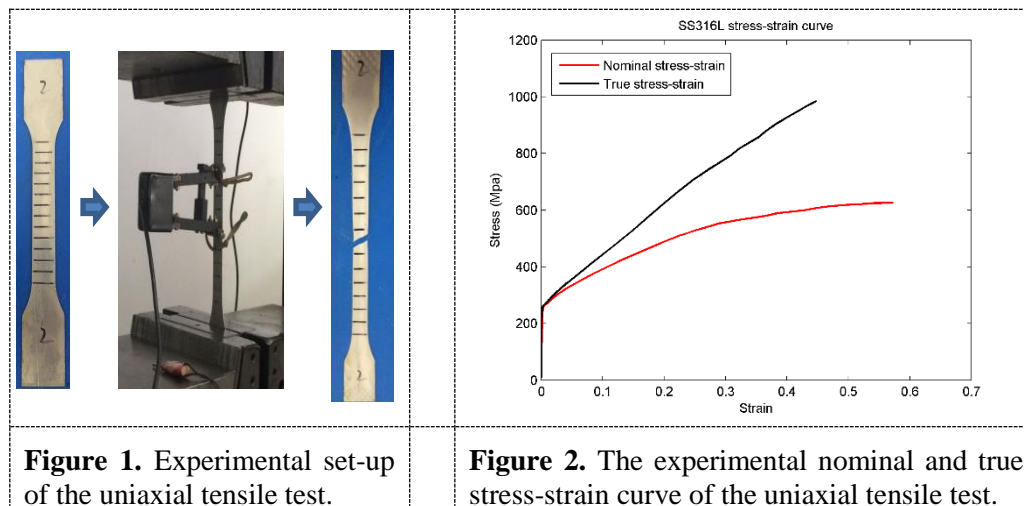


Figure 1. Experimental set-up of the uniaxial tensile test.

Figure 2. The experimental nominal and true stress-strain curve of the uniaxial tensile test.

2.3. Small punch test

The small punch test is performed with an MTS-E43 electro servo testing machine. The rod and the ball is driven by the testing machine and deforming the clamped disk sample, while the load and the deflection of the rod are recorded. The schematic of the SPT device is shown in figure 3, the punch is a 0.5mm radius ball, the upper die hole diameter is 1.05mm, the lower die hole diameter d is 1.5mm and the specimen is a TEM sample (3mm diameter disc and its thickness B is varying from 0.1 to 0.3 mm). The rod is made of low carbon steel with Elastic modulus of 210GPa and the punch ball is a ceramic ball with Elastic modulus of 300GPa. The top of the rod is flat and have a surface contact with

the ball during the test. A constant punch velocity of 0.2mm/min is used to perform the test. In order to remove the effect of the roughness on the experiment, the surfaces of the sample are polished.

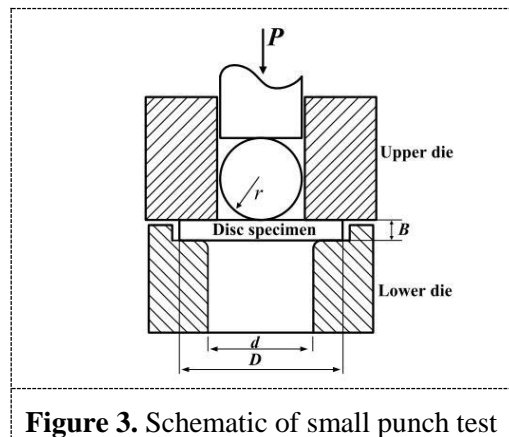


Figure 3. Schematic of small punch test

3. Finite element modelling of SPT

3.1. Traditional FEM model

The finite element model of small punch test is developed using ABAQUS 6.14-2 standard. The ball punch, lower die and upper die are modelled as rigid bodies shown in figure 4. The sample disc is modelled with CAX4R element, and the von Mises yield criterion is adopted. A friction coefficient of 0.2 is employed between the upper (lower) die and disc sample, while the no friction is assumed between the puncher and the sample. The input material properties from the uniaxial tensile test are used, Young's modulus E is 205GPa and the Poisson's ratio ν is 0.33. The plastic strain and the corresponding flow stress is calculated by the equation 1.

$$\varepsilon_{pl} = \varepsilon - \sigma/E \quad (1)$$

Where ε_{pl} is true plastic strain, ε is the true strain, and σ is the true stress. A series of ε_{pl} and σ pairs are input of the ABAQUS plastic parameters. The experimental load-deflection curves and FEM modelling result with and without loading system compliance corrected are shown in figure 5.

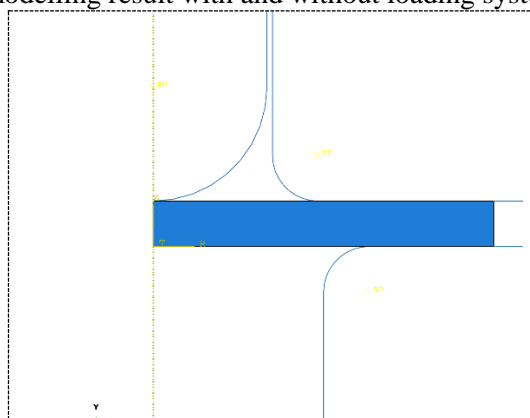


Figure 4. Traditional FEM set-up of the SPT

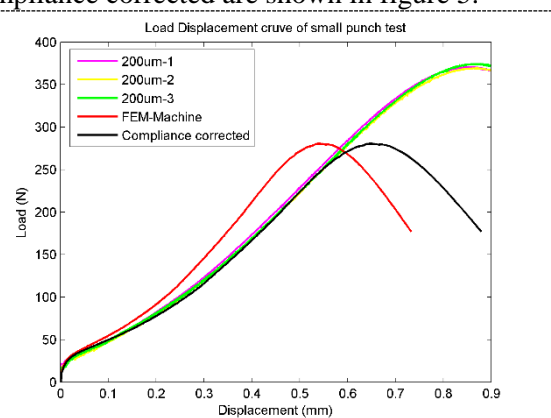


Figure 5. Experimental and FEM SPT load-deflection curves.

Three experimental results show good repeatability. The misalignment of the experimental and FEM results become larger as the displacement (Load) increase, the FEM (red line) load-deflection curve is much steeper than the experiment curves indicate that some system deformations are not included in the finite element calculation. The U_{max} for the experimental curves is higher than that of the FEM

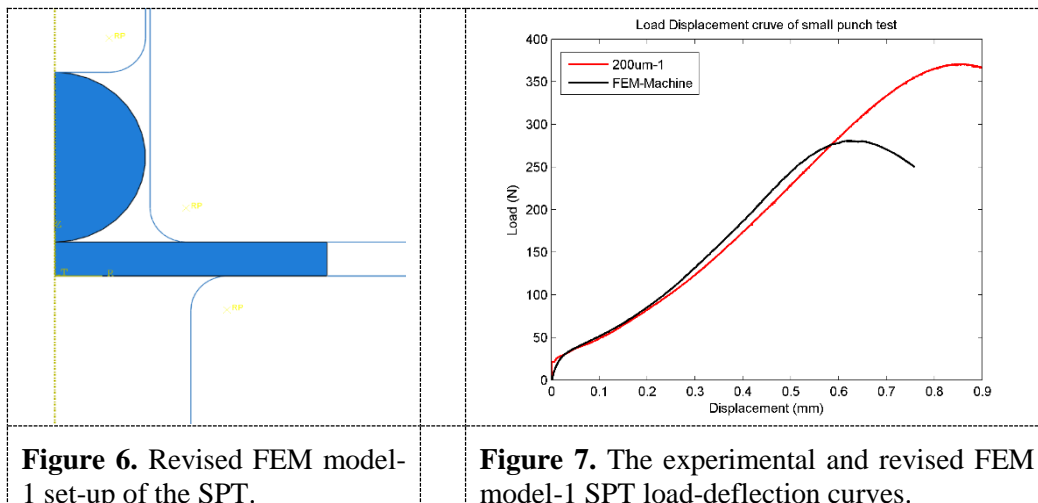
results, but we only focus on the horizontal misaligned. Compitelli[5] corrected the FEM simulation curve by adding the elastic displacement of the system through equation 2.

$$d_{sp} = d_{measure} - P/K \quad (2)$$

Where d_{sp} is the target displacement, the $d_{measure}$ is the displacement measured by the extensometer, P is the load and the K is the compliance of the loading system. They got good alignment with this method shown in black curve in figure 5, but K differs in different experiment. Note that no constitute relation extrapolation is performed, the maximum height of the experimental and FEM results differs in maximum height and this phenomenon is beyond the scope of this paper.

3.2. Revised FEM model-1

We revised the FEM modelling by adding sphere puncher into SPT set-up shown in figure 6, the ceramic ball is modelled as elastic ball with Young's modulus $E=300\text{GPa}$ and Poisson's ratio $\nu = 0.27$, the plastic properties of the ball is $\epsilon_{pl} = 0.2, \sigma = 800$ and $\epsilon_{pl} = 0.4, \sigma = 1200$. The results of the revised FEM model-1 and the experiment load-deflection curve is shown in figure 7.



The revised model-1 still differs from the experimental result and is not much different from the original model, since the ceramic ball is harder than the material and there is hardly any deformation during the test.

3.3. Revised FEM model-2

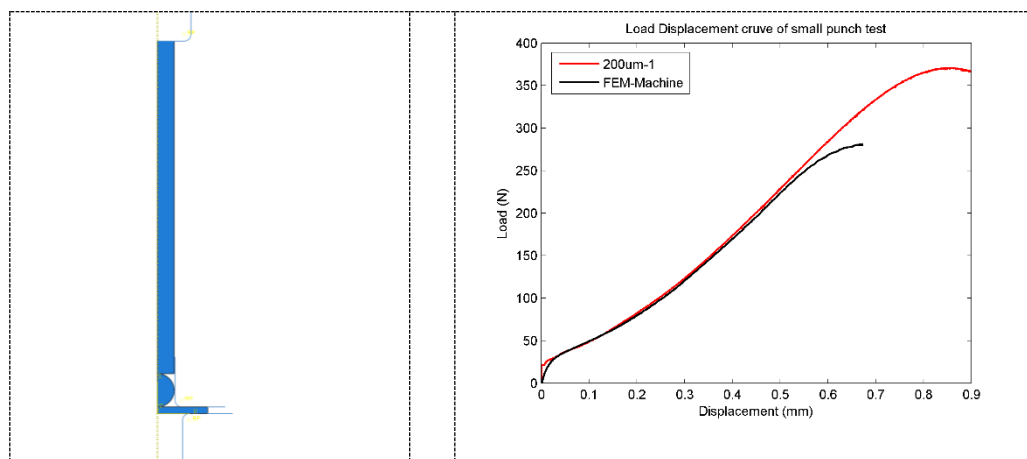


Figure 8. Revised FEM model-2 set-up of the SPT.

Figure 9. The experimental and revised FEM model-1 SPT load-deflection curves..

We revised the FEM model-1 by adding steel rod into SPT set-up shown in figure 8, the ceramic ball is modelled as revised FEM model-1 and the rod is 1mm in diameter and 35mm in height, modelled as Q345 low carbon steel with Young's modulus $E=206\text{GPa}$, Poisson's ratio $\nu = 0.3$ and the yield stress $\sigma_y = 345\text{MPa}$.

The results of the revised FEM model-2 and the experiment load-deflection curve is shown in figure 9. The revised model-2 alignment well with the experimental result except the misalignment with the height of the curve, this phenomenon might be solved by extrapolation of the constitutive relation of the testing material, will be discussed elsewhere. The ceramic ball puncher do not deform during the test and the loading system error is mainly from the elastic and plastic deformation of the rod. It is important to notice that the elastic compression of the rod is much smaller than the maximum loads difference of the FEM model and the experimental results. The difference come from the plastic deformation of the rod shown in figure 10, and the issue is observed in our experiment.

In order to avoid the plastic deformation we recommend the use the rod after plastic deformation instead of rounded rod surface, since the rounded rod made of steel might be worn after several experiment and the ceramic ball has good friction and wear property.

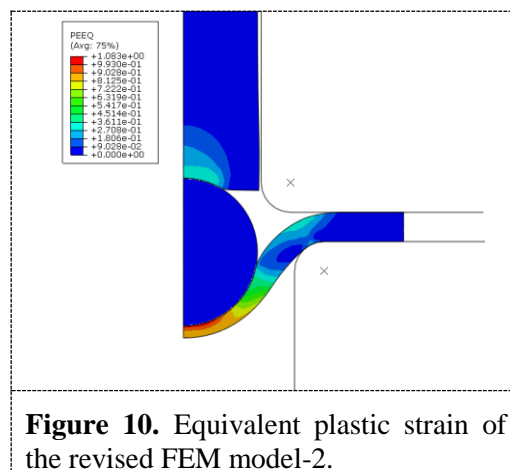


Figure 10. Equivalent plastic strain of the revised FEM model-2.

4. Conclusions

The rod plastic deformation during the small punch test can not be ignored, where the compliance of the loading system is relatively small compared to the plastic deformation of the rod. The rod and the sphere ceramic ball must be modelled of our loading system.

5. References

- 1.Mao, X. and H. Takahashi. Journal of Nuclear Materials, 1987. **150**(1): p. 42-52.
- 2.Murty, K.L. and I. Charit. Journal of Nuclear Materials, 2008. **383**(1–2): p. 189-195.
- 3.Ha, J.S. and E. Fleury. International Journal of Pressure Vessels & Piping, 1998. **75**(9): p. 707-713.
- 4.Lucas, G.E.,1983. **117**(8): p. 327-339.
- 5.Moreno, M.F., Materials & Design, 2018. **157**: p. 512-522.
- 6.Campitelli, E.N., et al., Materials Science & Engineering A, 2005. s **400–401**(1): p. 386-392.
- 7.Campitelli, E.N., et al., Journal of Nuclear Materials, 2004. **335**(3): p. 366-378.

Acknowledgments

This work is support by The National Key Basic Research Program (2017YFB0702202) and National Natural Science Foundation of China (U1532262).